FUNDAMENTALS & APPLICATIONS

CHEMELECTROCHEM

ANALYSIS & CATALYSIS, BIO & NANO, ENERGY & MORE

Accepted Article

Title: On the mechanism of scanning electrochemical potential microscopy

Authors: Jochen Friedl, Jingying Gu, Ulrich Stimming, and Ben Horrocks

To be cited as: *ChemElectroChem* 10.1002/celc.201701031

Link to VoR: http://dx.doi.org/10.1002/celc.201701031

A Journal of

ChemPubSoc Europe

WILEY-VCH

www.chemelectrochem.org

10.1002/celc.201701031

On the mechanism of scanning electrochemical potential microscopy

Dr Jochen Friedl, Dr Jingying Gu, Prof Ulrich Stimming and Dr Benjamin R. Horrocks[1]

School of Natural and Environmental Sciences, Bedson Building, Newcastle University, Newcastle upon Tyne, NE1 7RU, UK.

06/10/2017

Abstract

Scanning electrochemical potential microscopy (SECPM) is a type of probe microscopy in which a sharp tip similar to those employed in electrochemical tunnelling microscopy is connected to a high impedance amplifier, but the tip potential instead of tip current is used as the signal in the feedback loop. SECPM has been found to provide much higher spatial resolution than would be expected on the basis of a mechanism in which the tip responds to the local electrochemical potential of the solution; in fact it can obtain atomic resolution similar to STM, but is a superior technique for imaging electronically insulating objects such as proteins on a metal surface. We suggest a mechanism for these high resolution images based on electron exchange between tip and substrate coupled to faradaic processes at the tip/solution interface. This mechanism operates alongside the conventional mechanism in which the tip responds to the local potential in the diffuse layer of the substrate and allows a simple description of the sigmoidal tip potential-distance curves which have been reported.

Scanning electrochemical potential microscopy (SECPM) involves a small metal tip rastered over the surface of the sample in a manner similar to electrochemical scanning tunneling microscopy (EC-STM). The tip is typically insulated so that only the apex is wetted by the electrolyte, but in contrast to EC-STM the signal that is used to form the image is the tip potential, which is measured against a conventional reference electrode in the bulk solution (or the substrate) using a high input impedance amplifier [1]. In principle SECPM allows direct measurements of the electric double layer, but it is also of wider interest because it is capable of much higher lateral spatial resolution than originally expected and comparable to STM [2,3]. In particular, molecularly-resolved images of enzymes adsorbed to metal substrates have been obtained under conditions where EC-STM fails [4]. Building on some of the ideas of Traunsteiner et al.[5] we show that SECPM imaging can be understood on the basis of the interplay between tunneling and faradaic tip currents, but that there is no requirement to invoke leakage currents in the high impedance amplifier used.

As a metal tip approaches a metallic substrate at open circuit, the tip potential will be affected by the double layer at the substrate. This effect occurs over a range of tip/substrate separations of the order of the Debye length. If the ionic strength is high, then the tip must approach much closer in order to detect any difference between the local potential and the potential in bulk solution. For an aqueous solution of dimensionless ionic strength 0.1, corresponding to typical concentrations of inert electrolyte in voltammetric experiments (0.1 mol dm^{-3}), the Debye length is about 1 nm at ambient temperature. At 0.001 mol dm^{-3} this rises

[1] email:b.r.horrocks@ncl.ac.uk

to 10 nm, but it is still clear that the tip must (i) approach close to the substrate and (ii) must itself be of smaller vertical dimension. This places severe constraints on the tip insulation to achieve high resolution in SECPM simply by sensing the local potential in the double layer. Although the radius of curvature of the tip may be very small, the wetted area of the tip is determined by the extent to which the tip apex protrudes from the insulator. In electrochemical STM this is less of a constraint because all that is necessary is that the faradaic background is small with respect to the tunneling current from the apex of the tip. However, if SECPM operates by sensing the local potential, the whole wetted area of the tip is active and it is difficult to understand how molecularly-resolved images can be obtained.

We describe an additional mechanism that can explain the high resolution images obtained by SECPM; this mechanism is postulated to operate alongside the usual mechanism not instead of it. The basis of the mechanism is the observation that the high input impedance of the tip amplifier in SECPM does not preclude a contribution of tunneling to the signal, it only precludes the flow of charge from the tip to the external circuit. As the tip approaches close to the substrate electrons tunnel, as in STM, until the tip attains a potential at which the Fermi levels of tip and substrate are equal. The potential of the tip under this condition is a contact potential which is determined by the substrate [5]. Clearly, another process must be present to allow discharge of the tip capacitance if the system is to be capable of responding to variations of the tip/substrate distance during the image raster scan. Typically noble metal tips are employed in SECPM and even in bulk solution, far from the substrate, their potential is not poised by a well-defined half reaction via the Nernst equation. Instead the typical situation is that a mixed potential exists in which the potential at which zero net current flows is set by a balance between different anodic and cathodic reactions. The anodic process is likely to be oxidation of the metal surface and the cathodic processes may be reduction of oxygen or protons present in the solution. In the model developed below the tip capacitance discharges via the faradaic resistance associated with these reactions. For completeness, we also include the possibility of a non–zero input current (leakage current) at the amplifier, but this is not an essential part of the model. The rate of change of charge Q on the tip is given simply by the sum of the tunneling, faradaic and leakage currents by eqn (1):

$$-\dot{Q} = i_t + i_F + i_{inp} \qquad (1)$$

We can illustrate the operation of this imaging mechanism in a simplified case by assuming that the i–E characteristics for the tunneling and faradaic processes are in the linear regime near equilibrium.

$$-\frac{\partial}{\partial t}\int C dE = \frac{E(z)-E_c}{R_t} + \frac{E(z)-E_m-\varphi(z)}{R_F} + \frac{E(z)}{R_{inp}} \qquad (2)$$

10.1002/celc.201701031

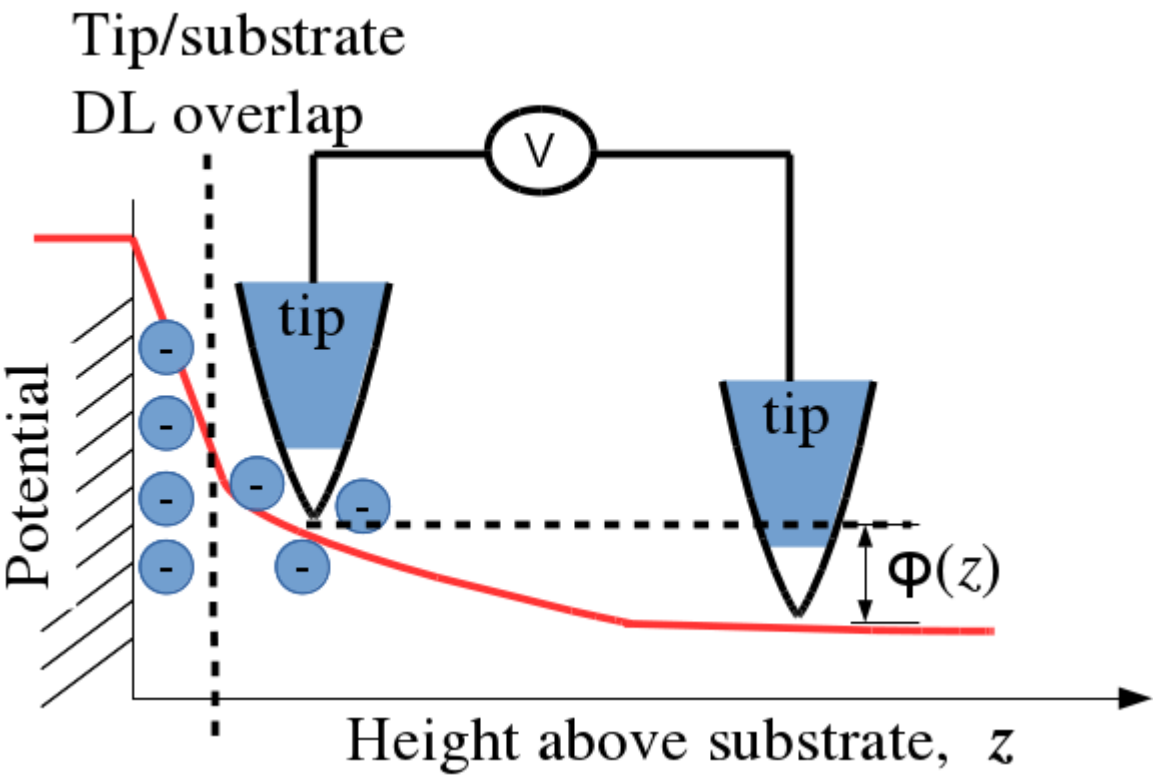

Figure 1: Schematic diagram of the variation of electric potential (red line) above a substrate electrode and the meaning of the term φ(*z*). In the absence of charge transfer with the substrate, φ(*z*) is simply the potential difference a perfect electrometer would measure between a tip at height *z* and another in the bulk solution. φ(*z*) is not the same as the local electric potential because (i) the tip and substrate double layers overlap and (ii) it represents an average over the wetted area of the tip (white). For an ideal, sharp tip, φ(*z*) approaches the local electric potential which may be estimated from standard theories of the double layer.

C is the differential capacitance of the tip. R_t is the tip/substrate gap tunneling resistance and E_c is the contact potential discussed previously [5]. For a perfectly sharp tip, φ(*z*) is simply the micropotential in the electric double layer at the substrate, however, for finite tips, it should be calculated by more sophisticated approaches which take into account tip/substrate double layer interactions [6,7]. In this work, we will approximate φ(*z*) by the standard Gouy–Chapman–Stern theory for the sake of simplicity, but the model which we describe does not rely on any particular functional form for φ(*z*). Fig. (1) illustrates schematically the meaning of φ(*z*). E_m is the mixed potential of the tip in bulk solution (or the Nernstian potential if it is poised by a simple redox couple) and R_F is the faradaic impedance (assumed time-independent for simplicity). We also include the leakage term, but the input impedance of the amplifier R_{inp} can exceed 10^{15} Ω and this term may be negligible. It is also possible, depending on the details of particular instrumentation, that leakage currents in the amplifier go via the substrate rather than to earth. In such a case R_{inp} is in parallel to R_t and equation (2) still applies, but with a modified tunneling resistance $R_t^* = \frac{R_t R_{inp}}{R_t + R_{inp}}$ and the third term on the right is omitted.

At steady-state the SECPM tip potential as a function of tip height, the approach curve *E*(*z*), is given simply by eqn (3):

$$E(z) = \frac{R_\parallel}{R_t} E_c + \frac{R_\parallel}{R_F}\left(E_m + \varphi(z)\right) \qquad (3)$$

Where $\frac{1}{R_{\|}} = \frac{1}{R_t} + \frac{1}{R_F} + \frac{1}{R_{inp}}$. This allows a simple calculation of the sigmoidal *E*–*z* curves that have been observed [1,5,6,8]. To illustrate this, we model the tunneling resistance as a simple exponential with inverse distance parameter β = 10 nm^{-1}, $R_t = R_t^0 \exp(\beta z)$ and we model φ(*z*) with a linear potential drop within the Helmholtz layer up to 0.25 nm and an exponential behaviour in the diffuse layer ($\varphi(z) = \varphi_{OHP} \exp(-\kappa[z - z_{OHP}])$. We also choose E_m as a reference potential and throughout measure potentials against E_m for simplicity. Fig. (2) shows a typical sigmoidal curve calculated from eqn (3) using reasonable values of the parameters.

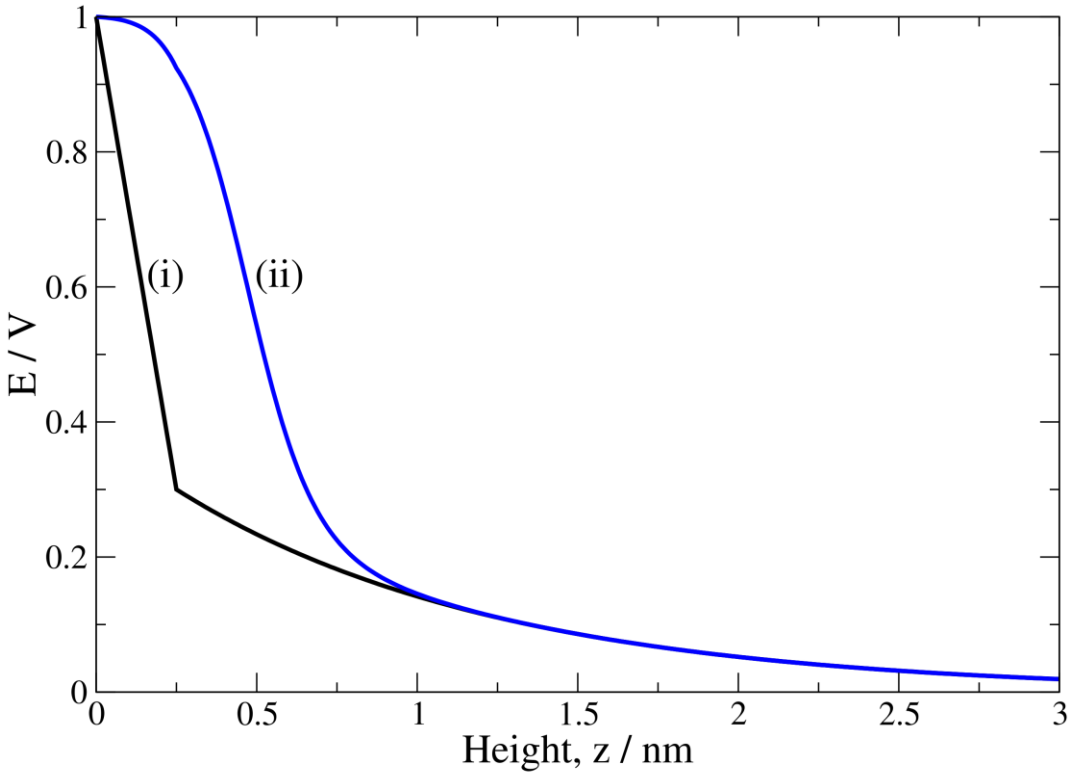

Figure 2: Calculated potential *E* as a function of height *z* above the substrate. (i) The local electric potential φ(*z*) in the substrate double layer according to Gouy–Chapman–Stern theory calculated using the linear Poisson-Boltzmann equation for the diffuse layer. (ii) The potential determined in an SECPM experiment *E*(*z*) calculated from the local electric potential φ(*z*) and equation (3). The parameters used in the calculation were: inverse tunneling length β = 10 nm^{-1}; inverse Debye length κ = 1 nm^{-1}; E_c = 1 V; R_t = 1 *G*Ω; R_F = 100 *G*Ω and R_{inp} = 10^{15} Ω.

If the amplifier input impedance is so great it may be neglected, $R_{inp} \gg \frac{R_t R_F}{R_t + R_F}$, the measured potential in SECPM is strictly greater than the local electric potential *E*(*z*) > φ(*z*). This remains true even if a more sophisticated analysis of φ(*z*) is made [6,7]. For sufficiently large leakage currents and for sufficiently large distances, the measured potential *E* may be less than φ, but the shape of the curve is still sigmoidal as can be seen by examining the form of eqn (3). It is worth noting that the SECPM approach curve is also rather insensitive to φ(*z*) at small tip/substrate distances and this is why *E*(*z*) appears smooth even where φ(*z*) is not.

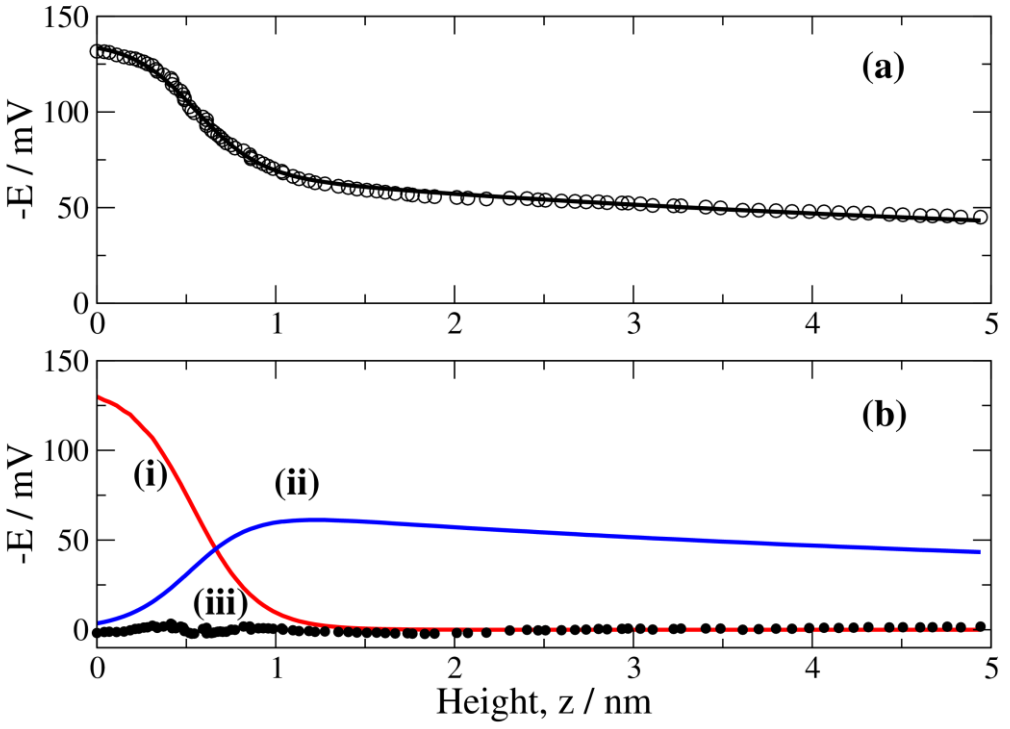

Figure 3: Least squares fit of equation (3) to experimental data for potential E against height z determined in an SECPM experiment with an Au(111) substrate at -0.8 V against Au/Au oxide in 10^{-4} mol dm^{-3} H_2SO_4 and an Au tip. (a) Experimental tip potential (symbols) and fitted regression model (line). (b) (i) The contribution of tunneling $\frac{R_\parallel}{R_t}E_c$ and (ii) of the local electric potential $\frac{R_\parallel}{R_F}\varphi(z)$ to the measured tip potential according to the fit in (a). (b)(iii) Residual for the fit in (a); maximum absolute deviation = 3.4 mV. The best fit parameters were: inverse tunneling length $\beta = 5.58$ nm^{-1}; $E_c = -0.136$ V, $R_t^0 = 2.28 \times 10^{13}$ Ω and $R_F = 8.44 \times 10^{14}$ Ω. The inverse Debye length was fixed at $\kappa = 0.0574$ nm^{-1} and the amplifier input impedance was fixed as $R_{inp} = 10^{15}$ Ω.

A suitable regression model for the analysis of experimental data is obtained by combining equation (3) with an expression for the local electric potential in the double layer. We used the standard expression given by equation (4):

$$\frac{\tanh(f\varphi/4)}{\tanh(f\varphi_2/4)} = e^{-\kappa z} \qquad (4)$$

where $f = F/RT$ and φ_2 is the potential at the outer Helmholtz plane. The details of the potential in the inner layer for $0 < z < z_{OHP}$ are unimportant because in this region $\varphi(z)$ hardly affects the final value of $E(z)$. The reason for this is that the tunneling contribution to E dominates for $z < 1$ nm.

Figure 3a shows a fit of the regression model defined by equations (3) and (4) to experimental data obtained with an Au tip above an Au(111) substrate poised at -0.8V w.r.t. Au/Au oxide in 10^{-4} mol dm^{-3} H_2SO_4. For clarity, the data is presented as $E(z)$ defined as in equations (2) & (3) using the value of E_c determined from the fit even though the actual raw

potential data tends to zero as $z \rightarrow 0$, i.e., is in the form E_c - E. The inverse tunneling decay length β was floated in the regression, but the inverse Debye length was calculated to be 0.0574 nm^{-1} on the assumption that H_2SO_4 is fully dissociated under the experimental conditions (its second pK_a is about 2.0). The electrometer input impedance was fixed at 10^{15} Ω and the faradaic impedance was allowed to float as were φ_2 and R_t^0. As $z \rightarrow 0$, $E \rightarrow E_c$ and $\frac{\partial E}{\partial z} \rightarrow 0$, therefore the exact location of $z = 0$ is uncertain and therefore the value of R_t^0 is probably overestimated because our fitting procedure assumes $z = 0$ at the point of closest approach in the data. Using typical tip size estimates [6,7], $R_F = 8.44 \times 10^{14}$ Ω corresponds to an exchange current density of about 2.5 μA cm^{-2} which is a typical order of magnitude for background currents at noble metal electrodes. The data indicates the substrate is biased negative of the pzc and therefore a cathodic faradaic process at the tip such as oxygen or proton reduction is most likely responsible for sustaining the tunneling of electrons between the substrate and the tip.

Figure 3b shows the contributions of the tunneling effect (the first term in equation (3)) and of the local electric potential in the diffuse layer (second term in equation (3)) determined from the fit shown in figure 3a. It is clear that for $z < 1$ nm, the SECPM is operating much like an STM and the technique only responds directly to the local electric potential when $\beta z \gg 1$ and the tip/substrate tunneling resistance is much greater than the faradaic resistance. In figure 3a this region is visible in the experimental data as a gradual decay in E for $z > 1$ nm because the Debye length is about 17 nm, much larger than the scan range (5 nm) and the tunneling decay length (β^{-1}), which was estimated to be about 0.18 nm.

The other important feature of figure 3a is the shape of the $E(z)$ curve in the tunneling region $z < 1$ nm; if this were interpreted as a local electric potential, the curvature of $E(z)$ would correspond to a local charge density of the same sign as that on the substrate. This is clearly unphysical and adds weight to the argument that in this region the SECPM tip is operating as a potentiometric form of STM and not as a sensor for the potential.

In order to understand the SECPM imaging mechanism, we must consider the time-dependent eqn (2). As the tip rasters across the substrate the tip/substrate height z changes. Normally the SECPM is operated with a feedback loop that uses a fixed value of E relative to the substrate as the setpoint, however we treat the case where the value of E is allowed to fluctuate because the operation of the feedback loop is standard and not of primary interest here. A small change in tip–substrate height δz induces a small change in measured potential δE which can be obtained by a Fourier analysis of eqn (2).

$$\frac{\delta E}{\delta z} = \frac{\frac{R_\parallel}{R_t}\beta(E-E_c)+\frac{R_\parallel}{R_F}\phi}{1+j\omega C R_\parallel} \qquad (5)$$

The response of the tip potential to variations in height δz is governed by $R_\parallel C$ and for $\omega R_\parallel C \ll 1$ the gradient of the dc limit illustrated in Figs. (2) & (3) applies. As the tip approaches within tunneling range, electrons tunnel between tip and substrate; this charges the tip double layer capacitance and the tip discharges through the faradaic resistance as it moves away from the surface. This charging/discharging process must be rapid in order for the tip to respond correctly as it passes rapidly over small protrusions during a raster scan. Using the dimensions of the tips simulated by Hamou et al.[6,7] the wetted area A is about 1200 nm^2 and taking $\frac{C}{A} \simeq 20$ μF cm^{-2}, simple estimates of $R_\parallel C$ show that it is sufficiently small (order of *ms* for $z < 1$ nm using the parameters of Fig. (3)) to be compatible with the use of SECPM as a scanning probe imaging technique. The form of eqn(5) also suggests that information on $\varphi'(z)$ can be obtained by modulating the tip height because $\varphi'(0) > 0$. Finally, we note that slow variations in E have been reported (order of seconds) [1]. These are not predicted by our model for reasonable values of the parameters, however they are likely to be related to slow time–dependent faradaic processes which we did not include explicitly.

SECPM tip potentials comprise three contributions (i) the local electric potential averaged over the tip and modified for tip/substrate double layer interaction, (ii) a potential arising from exchange of electrons with the substrate through the tunneling resistance and (iii) a potential arising from leakage currents in the amplifier. These mechanisms are independent of each other – any or all may contribute to the measured signal, depending on the magnitudes of the faradaic resistance, tunneling resistance and input impedance of the amplifier. If measurements of the local potential $\varphi(z)$ are desired, then the faradaic resistance should be minimised by incorporating a suitable redox couple at the tip. In the case where the amplifier input impedance is infinite, the tunneling contribution still occurs because the tip double layer capacitance can discharge through the faradaic impedance and it is not necessary for any current to flow into the amplifier to sustain tunneling. Finally, we note that the high resolution SECPM images that have been reported are consistent with the tunneling aspect of the mechanism and that SECPM may function as an extremely low current version of STM which may be particularly suited to imaging high resistance objects, e.g., large proteins adsorbed on a metal surface.

Experimental

Scanning electrochemical microscopy (SECPM) approach curves were measured using a Multimode 8 SECPM (Bruker). The substrate was a film of Au on borosilicate glass oriented as Au(111) (Arrandee Metal GmbH, Germany), and it was annealed using a butane gas burner before use. The SECPM tip was prepared from a 0.25 mm Au wire (Goodfellow Cambridge Ltd, UK). The tip was cut manually and then coated with nail polish. Upon drying in a vertical orientation, only a region close to the apex is exposed. The electrolyte was 10^{-4} mol dm^{-3} H_2SO_4(aq) and the reference electrode was Au/Au oxide. To measure approach curves, the tip was brought near to contact with the substrate at -0.8 V by decreasing the setpoint to about 5 mV and then retracted 5 nm at a scan rate of 0.5 nm s^{-1}. The laboratory temperature was about 20^{o}C.

Keywords

Faradaic, potential, probe microscopy, SECPM, tunneling.

References

[1] C. Hurth, C. Li, A. J. Bard, *J. Phys. Chem. C* **2007**, *111*, 4620–4627.

[2] M. Herpich, J. Friedl, U. Stimming in *Surface Science Tools for Nanomaterials Characterisation* (Ed. C. S. S. R. Kumar), Springer-Verlag, Berlin, Heidelberg, **2015**, pp. 1–67.

[3] H. Wolfschmidt, C. Baier, S. Gsell, M. Fischer, M. Schreck, U. Stimming, *Materials* **2010**, *3*, 4196–4213.

[4] C. Baier, U. Stimming, *Angew. Chem. Int. Ed.* **2009**, *48*, 5542–5544.

[5] C. Traunsteiner, K. Tu, J. Kunze-Liebhäuser, *ChemElectroChem* **2015**, *2*, 77–84.

[6] R. F. Hamou, P. U. Biedermann, A. Erbe, M. Rohwerder, *Electrochim. Acta* **2010**, *55*, 5210–5222.

[7] R. F. Hamou, P. U. Biedermann, A. Erbe, M. Rohwerder, *Electrochem. Commun.* **2010**, *12*, 1391–1394.

[8] Y.-H. Yoon, D.-H. Woo, T. Shin, T. D. Chung, H. Kang, *J. Phys. Chem. C* **2011**, *115*, 17384–17391.